

AD-A243 850



2

TECHNICAL REPORT BRL-TR-3304

BRL

DTIC
ELECTE
JAN 06 1992
S D

**ELECTRICAL ENERGY SHAPING FOR
BALLISTIC APPLICATIONS IN
ELECTROTHERMAL GUNS**

**G. L. KATULKA
H. BURDEN
A. ZIELINSKI
K. WHITE**

DECEMBER 1991

92-00140

APPROVED FOR PUBLIC RELEASE; DISTRIBUTION IS UNLIMITED.

U.S. ARMY LABORATORY COMMAND

**BALLISTIC RESEARCH LABORATORY
ABERDEEN PROVING GROUND, MARYLAND**

NOTICES

Destroy this report when it is no longer needed. DO NOT return it to the originator.

Additional copies of this report may be obtained from the National Technical Information Service, U.S. Department of Commerce, 5285 Port Royal Road, Springfield, VA 22161.

The findings of this report are not to be construed as an official Department of the Army position, unless so designated by other authorized documents.

The use of trade names or manufacturers' names in this report does not constitute indorsement of any commercial product.

REPORT DOCUMENTATION PAGEForm Approved
OMB No. 0704-0188

Public reporting burden for this collection of information is estimated to average 1 hour per response, including the time for reviewing instructions, searching existing data sources, gathering and maintaining the data needed, and completing and reviewing the collection of information. Send comments regarding this burden estimate or any other aspect of this collection of information, including suggestions for reducing this burden, to Washington Headquarters Services, Directorate for Information Operations and Reports, 1215 Jefferson Davis Highway, Suite 1204, Arlington, VA 22202-4302, and to the Office of Management and Budget, Paperwork Reduction Project (0704-0188), Washington, DC 20503.

1. AGENCY USE ONLY (Leave blank)		2. REPORT DATE December 1991	3. REPORT TYPE AND DATES COVERED Final, Nov 89 - Sep 90	
4. TITLE AND SUBTITLE Electrical Energy Shaping for Ballistic Applications in Electrothermal Guns.			5. FUNDING NUMBERS 1F279W9X DG53 DA31880	
6. AUTHOR(S) G. L. Katulka, H. Burden, A. Zielinski, K. White				
7. PERFORMING ORGANIZATION NAME(S) AND ADDRESS(ES)			8. PERFORMING ORGANIZATION REPORT NUMBER	
9. SPONSORING / MONITORING AGENCY NAME(S) AND ADDRESS(ES) U.S. Army Ballistic Research Laboratory ATTN: SLCBR-DD-T Aberdeen Proving Ground, MD 21005-5066			10. SPONSORING / MONITORING AGENCY REPORT NUMBER BRL-TR-3304	
11. SUPPLEMENTARY NOTES				
12a. DISTRIBUTION / AVAILABILITY STATEMENT Approved for public release; distribution is unlimited.			12b. DISTRIBUTION CODE	
13. ABSTRACT (Maximum 200 words) A five-stage, 130-kJ pulse forming network (PFN) for delivering electrical energy to an experimental ETC gun is described. The device is fundamentally a network of RLC circuits where the load, R, is either a fixed-metallic or variable-plasma resistance. Capacitors provide long-term energy storage, inductors are used for pulse shaping, ignitrons are used as closing switches, and power diodes serve as "clamping" diodes to protect the capacitors from voltage reversal during operation. Linear theory network simulations of circuit discharge into the fixed load within an energy range of 1.4 to 22.0 kJ are in close agreement with experiment. Resistance measurements of plasmas generated using this PFN indicate that plasma resistance is a strong function of current. It is linear with capillary length and inversely proportional to capillary diameter. Loss of diodes during operation was frequent. The probable cause of this problem and circuit revisions to reduce diode stresses are described.				
14. SUBJECT TERMS electrothermal-chemical; ETC; plasma; pulse power; pulse forming network; PFN; electric power; electrical impedance			15. NUMBER OF PAGES 21	
			16. PRICE CODE	
17. SECURITY CLASSIFICATION OF REPORT UNCLASSIFIED	18. SECURITY CLASSIFICATION OF THIS PAGE UNCLASSIFIED	19. SECURITY CLASSIFICATION OF ABSTRACT UNCLASSIFIED	20. LIMITATION OF ABSTRACT UL	

INTENTIONALLY LEFT BLANK.

TABLE OF CONTENTS

	<u>Page</u>
LIST OF FIGURES	v
LIST OF TABLES	vii
1. BACKGROUND	1
2. PROCEDURE	2
3. CONCLUSIONS	8
4. REFERENCES	17
DISTRIBUTION LIST	19



Accession For	
NTIS CR4&I	<input checked="" type="checkbox"/>
DTIC TAB	<input type="checkbox"/>
Unannounced	<input type="checkbox"/>
Justification	
By	
Distribution/	
Availability Codes	
Dist	Avail and/or Special
A-1	

INTENTIONALLY LEFT BLANK.

LIST OF FIGURES

<u>Figure</u>	<u>Page</u>
1. The 130-kJ Power Supply Used at BRL for ET Gun Studies	9
2. Current Profiles of Modules 1-5 With Switching at $t = 0, 280 \mu s, 370 \mu s, 597 \mu s,$ and $741 \mu s$, Respectively. Solid Line Indicates Total Load Current . . .	9
3. Power Profiles of 13-kJ Discharge to a 35-Milliohm Load	10
4. Energy Profiles of 13-kJ Discharge to a 35-Milliohm Load	10
5. Diagram of Electrothermal-Gun Capillary Chamber	11
6. Resistance Curves of a Capillary With Length = 52.75 mm and Diameter = 9.45 mm	11
7. Resistance vs. Current of the 22-kJ Test in Figure 6	12
8. Resistance Curves of Capillary With Length = 52.75 mm and Diameter = 12.3 mm	12
9. Resistance With Length = 97.2 mm and Diameter = 12.3 mm Compared to Scaled Figure 8	13
10. Two Module PFN With Second Module Triggered at $250 \mu s$. Circuit With a Diode Shunting Capacitor and Switch (a) and the Same Circuit With the Ignitron Extinguished (b)	13
11. Theoretical Plots of Inductor Voltage (V_L), Load Voltage (iR_L), and Diode Current for the Circuit of Figure 10a Without a Second Module (a) and With a Second Module (b)	14
12. Diagram of Circuit With the Ignitron Switch Moved and the Diode Directly in Parallel With the Capacitor	14
13. Measurement of Diode Current in Circuits With Two Degrees of Damping	15

INTENTIONALLY LEFT BLANK.

LIST OF TABLES

<u>Table</u>	<u>Page</u>
1. Power Peaks for Firing #1	3
2. Time to Power Peaks for Firing #1	3
3. Power Peaks for Firing #2	3
4. Time to Power Peaks for Firing #2	4
5. Experimental and Theoretical Plasma Resistances	5

INTENTIONALLY LEFT BLANK.

1. BACKGROUND

A pulse forming network provides a way of delivering a desired amount of stored electrical energy to a given load with a prescribed pulse shape. Networks that store energy in the form of an electrostatic field are voltage-fed networks, and they consist mainly of high energy capacitors that are rated for several kilovolts. The stored energy is directly related to the total capacitance of the circuit and the square of the initial voltage placed on that capacitance. A second type of network encompasses energy in a magnetic field by running electric current through large inductors. Here, the stored energy is related to the total inductance and the square of the current through the inductance, and it is called a current-fed network. Two advantages of a voltage-fed network are that the energy can be stored with small losses for a long period of time and the energy can be delivered to the circuit by operating a closing switch such as an ignitron or thyatron. For these reasons, the voltage-fed network has become a very common type of PFN (Glasoe and Lebacqz 1948). The PFN (see Figure 1) that is used to support electrothermal gun experimentation at the U.S. Army Ballistic Research Laboratory (BRL), Aberdeen Proving Ground, MD, is initially a voltage-fed network with a maximum energy storage capability of 130 kJ. When the diodes are conducting, the PFN becomes a current-fed network. It consists of five independently triggered, parallel modules, each of which contributes to the composite pulse that is delivered to the load. Clamping diodes are used in the circuit to protect the energy storage capacitors from voltage reversals. The initial quarter period of a module is the time required to reach the peak output power, and it is approximately given by the following:

$$t_{1/4} = (\pi/2) \cdot (L \cdot C)^{1/2}. \quad (1)$$

The values of L and C are, respectively, the total inductance and capacitance of a module. R is the resistance of the load. The impedance of each module is roughly given by the following:

$$Z = (L/C)^{1/2}. \quad (2)$$

The resultant current pulse is primarily dependent upon the values of L, C, the load resistance, and the closing time of each switch. The PFN was designed to provide a wide

flexibility in pulse shape over a 1-ms period. This was accomplished by staging four modules at nominally 250- μ s intervals. A fifth module was added later to initiate the capillary discharge. The analytical solution for each module current, assuming an underdamped network, was used to estimate circuit elements needed to achieve a desired load current-ramp waveshape. A typical current profile showing the individual module currents along with the total load current is given in Figure 2. In this case, the switches closed sequentially at times zero, 280 μ s, 370 μ s, 597 μ s, and 741 μ s. The modularity of the power supply allows for uncertainties in the capillary design. The power supply design process will not be presented here.

2. PROCEDURE

A general circuit analysis program, Micro-CAP^{*}, has recently been used to model the PFN discharge into a constant value load. It predicts the current, voltage, power, and energy waveforms of the discharging PFN. Simulations obtained using the software were compared to experimentally measured power and energy delivered to the load as a result of the PFN discharge.

In this first series of firings, a fixed resistance of 35 milliohms served as the load. The result of a particular discharge with the PFN initial energy at 13 kJ is shown in Figures 3 and 4. The experimental record of load power along with the corresponding simulation is shown in Figure 3, and the total energy delivered to the load is given in Figure 4. In the curves of Figure 3, five individual pulses, each the contribution of an individual LC module, can be identified. In this shot, the ignitron switches closed at the times as shown in Figure 2. The computed values of the quarter periods of the modules from Powell and Zielinski (unpublished) are 122 μ s, 169 μ s, 210 μ s, 140 μ s, and 130 μ s for modules 1 through 5, respectively. If the quarter period time is added to the time at which each switch is closed, the result should yield approximately the time at which the pulse comes to a peak. The peaks of both the experiment and simulation are in reasonable agreement. To help in comparing the simulation to the experiment, tables of the power peaks and the times at which they occur are given in Tables 1 and 2.

^{*}Micro-CAP is an electronic circuit analysis program created by Spectrum Software, 1021 S. Wolfe Road, Sunnyvale, CA.

Table 1. Power Peaks for Firing #1

Experiment	Simulation
6.3 MW	6.1 MW
2.8	3.1
7.5	7.9
16.6	12.9
33.1	32.1

Table 2. Time to Power Peaks for Firing #1

Experiment	Simulation
100 μ s	110 μ s
360	368
560	482
700	707
825	827

The results of a second firing that had an initial energy of 1.4 kJ and a different pulse shape than that of the first are given in Tables 3 and 4. The close agreement between experiment and simulation for these tests proved that the nonlinearities of circuit elements such as ignitrons were small; therefore, these elements can be represented by lumped parameters and produce, in most cases, discrepancies on the order of 2% or less.

Table 3. Power Peaks for Firing #2

Experiment	Simulation
0.70 MW	0.70 MW
0.28	0.35
0.74	0.85
1.7	1.4
2.7	2.8

Table 4. Time to Power Peaks for Firing #2

Experiment	Simulation
92 μ s	110 μ s
337	370
551	482
679	707
922	923

In succeeding firings, the fixed load was replaced by an electrothermal gun capillary chamber shown in Figure 5. The capillary chamber contains a fuse, having a width of 6 mm and thickness of 0.5 mm, passing longitudinally through a polyethylene tube, and connecting the high potential side of the PFN to ground. During a typical discharge of the PFN into the chamber, the fuse is vaporized by the electrical energy that passes through it, thereby forming a plasma inside the polyethylene tube. The main goal during this series of firings was to obtain voltage and current measurements of the capillary plasma so that an experimental resistance could be calculated. It is of interest to determine resistances of plasmas generated from capillaries with various energies and chamber configurations, since the plasma is serving as the load for the PFN. The load resistance is critical in determining the energy transfer efficiency. When the characteristic impedance of the PFN is matched to the load, a maximum power transfer will occur during the discharge, and current that flows through the load will damp rapidly. On the other hand, with the load resistance much less than the PFN, current through the load will be greater in magnitude, and it will take longer to damp. As a result, diodes must tolerate larger currents.

Current rate (di/dt) measurements were made with a Rogowski coil, and voltage measurements were made with a resistive string which is connected in parallel with the load and passes through a Pearson current transformer (model 110). All the measuring circuits utilized an inductive link providing a high degree of electrical isolation between the PFN and the data acquisition circuits. A mutual inductance of 0.3 μ H was measured between the leads of the voltage measuring circuit and the main circuit, which was taken into account when resistance curves were calculated. The accuracy of the resistance measuring circuit is estimated to be 5%.

*This value is based on an average sensitivity obtained from tests where the position of the conductor, with respect to the Rogowski axis, is varied and the conductor is normal to the plane of the coil to within 10° .

Timing of the PFN for all succeeding experiments was adjusted to switch the final four modules 100 μ s earlier—at 180 μ s, 270 μ s, 497 μ s, and 641 μ s, respectively. Resistances of three such firings are shown in Figure 6. (In all three firings, the prepulser bank had approximately the same stored energy.) A plot of resistance against current for one of these tests (see Figure 7) indicates that resistance is a strong function of current, but more importantly, it shows resistance to be a double-valued function of current. At a given current, the lower resistance curve applies when the current is increasing, and the higher curve applies when the current is decreasing (see Figure 2).

In another configuration, the capillary diameter was increased to 12.3 mm, and the length of the capillary was held at 52.75 mm. The resistance values are plotted in Figure 8. In this case, the resistances dropped from that in Figure 7 by roughly the ratio of the square of the capillary diameters. For a third configuration, the length of the capillary was increased by a factor of 1.84 to 97.2 mm, and its diameter was unchanged. The resistance is shown in Figure 9, along with the previous curve multiplied by 1.84. In comparison, the curves are similar in the lowest values achieved, thus illustrating the nearly linear dependence of resistance upon length in the range of this experiment.

The data in Table 5 compares experimental to theoretical values of resistance for a given amount of current. The experimental data points were taken from the resistance curve shown in Figure 8. The theoretical data is the result of a one-dimensional, steady-state computer model of plasma arcs (Powell and Zielinski, unpublished).

Table 5. Experimental and Theoretical Plasma Resistances

I (Peak)	R (Experimental)	R (Theoretical)
8.2 kA	84 milliohms	63 milliohms
5.3	130	89
18.3	47	36
28.4	32	28
47.6	21	20

Several times during the experiment, the clamping diodes of various modules were destroyed. These diodes (e.g., Figure 10a), which shunt the capacitor-ignitron leg of the circuit, characteristically conduct in only one direction—that defined when a positive voltage V is applied to the terminal marked "+". And, except for a negligible drop in the ignitron, the voltage applied to the diode is just equal to the capacitor voltage. Consequently, when the charge on the capacitor swings to a negative value, the diode begins to conduct, thus limiting any further charging of the capacitor. This is equivalent to placing a massive conductor (e.g., a "crowbar") across the capacitor-ignitron leg that "clamps" the voltage at zero. Crowbar diodes are needed to prevent damage to capacitors caused by reverse polarity swings. (Note in Figure 11a that the zero-charge, polarity reversal condition is nearly coincident with the time of peak of the current initiated by ignitron turn-on.)

Diode failure is usually a consequence of application of excessive reverse voltage, excessive forward current, a large turn-on di/dt , or a high reverse dv/dt across a conducting diode (Jamison, Stearns, and Fendley 1990). The first three points were considered in the design and operation of the PFN, but the fourth was less well understood. Analysis to disclose the cause of failure was concentrated on the new circuit (Figure 10b) existing after commencement of diode conduction. Here, energy stored in the inductor is now the only source sustaining current in the loop. We look at the performance of this loop, first alone and then as perturbed by the later discharge of a second bank into the load. If the diode-inductor-load loop alone is subjected to Kirchoff's requirement that the sum of voltages measured around any circuit be zero, we expect to find that the voltage, $L di/dt$, developed across the series inductor is negative (the Kirchoff convention for a source) and is equal in magnitude to the voltage, iR_L , developed in the load (Figure 11a). This constrains di/dt to be negative—which is to say, the current and consequently iR_L are decreasing. The rate of change of current is thus proportional to the current so that the decay is exponential—the current approaches a zero value asymptotically.

A new posture is created (Figure 11b) when a second module is fired into the load; the fresh source of energy drives added current to increase and maintain the voltage across the

*This reasoning is the same whether applied to negative or positive capacitor charge if diode polarity is adjusted accordingly. In the actual PFN, negative capacitor charging was most convenient but, in discussion, positive charging was more natural.

load. This, in consonance with Kirchoff's demand that inductor and load voltages sum to zero, dictates that the magnitude of negative voltage across the first loop's series inductor increases and persists. For simplicity, assume that the load voltage is maintained constant—now the opposing $L \, di/dt$ will become constant and somewhat increased in magnitude. The current is thus decreasing linearly and at a sharper slope, going steadily to zero and on into the negative (reversed flow) regime. The diode, still with an internal supply of current carriers, conducts the reversed flow briefly until the carrier supply is exhausted and then abruptly cuts off, producing a large positive di/dt . The inductor responds by generating a positive $L \, di/dt$ voltage in series with, and now aiding, the load voltage; the Kirchoff voltage equal and opposite to their sum is found across the diode's high resistance just as conduction is ceasing, which is a condition (Jamison and Stearns 1990) for the diode's destruction. This discussion assumes that the crowbar, in taking on total conduction, promoted complete extinction of the ignitron. Thus, later, when the storage capacitor might have buffered the destructive voltage surges applied to the diodes, it stands disconnected from the circuit (see Figure 10b).

If ignitron conduction losses can be tolerated over the full duration of the discharge cycle, the diodes may be connected directly across the capacitor bank and the ignitron switch relocated between the diode leg and the series inductor (Figure 12). In this new configuration, the storage capacitors remain connected to absorb reverse current flow, shunting it around the diode; the only limitation to this shunting is the small inductive impedance L_b of the diode-capacitor circuitry in the earliest portion of a transient. Their small inductance unfortunately works with the large capacitance to constitute an oscillatory circuit with extremely low characteristic impedance. Consequently, at the time when crowbarring is initiated, even the very small energy stored in the inductance will produce relatively large amplitude, oscillatory transients (Figure 13) that may damage the diode first by turning it on with a di/dt that exceeds the diode rating of $200 \, A/\mu s$. Second, if the load current is very rapidly damped (e.g., by rising load resistance), the negative going peaks of the rapidly oscillating capacitor current may drive the diode (whose current is a superposition of the capacitor circuit and the load circuit currents) to cutoff, simultaneously producing a destructive reverse-voltage rise. To forestall this, added inductance L_b and a few milliohm, series resistance R_b may be inserted in a capacitor lead (Figure 12); the resistance needed for near critical damping will be small and should absorb little main discharge energy during the

quarter cycle preceding crowbarring. Also, the inductance, whose nature is to sustain the current tending to charge the capacitor negatively, will slow the transfer of current to the diode, thus limiting its turn-on di/dt .

3. CONCLUSIONS

Nonlinearities in the PFN elements have been shown to be negligible by the agreement between experimental and simulation data. Simulations were necessary throughout the experiment for comparison purposes and for diagnostics when irregularities in the circuit occurred.

Our capillary chamber firing data indicate a strong dependence of plasma resistance upon magnitude of current. The data in Figures 6, 7, and 9 show that the resistance of a plasma is approximately an inverse function of the cross-sectional area of the capillary chamber and that there is a linear relationship between the plasma resistance and the capillary length. In a given shot, the resistance of a plasma is a double-valued function of current with its value depending upon a positive- or negative-going current.

Finally, when sequential discharges to a common load are used and closing switch losses can be tolerated, clamping diodes of the PFN should be placed directly in parallel with capacitors to avoid voltage transients. In addition, resistance should be added in the capacitor-diode circuit loop to damp unwanted current oscillations.

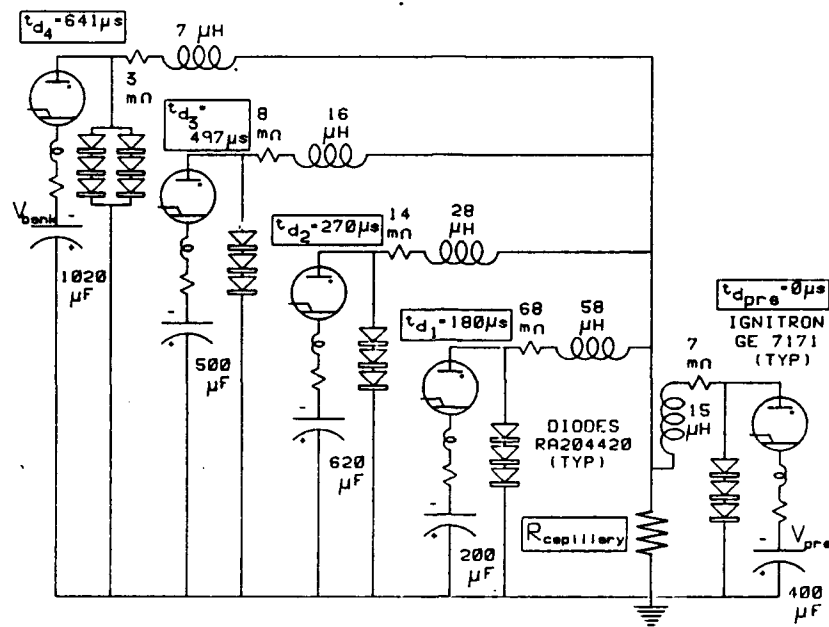


Figure 1. The 130-kJ Power Supply Used at BRL for ET Gun Studies.

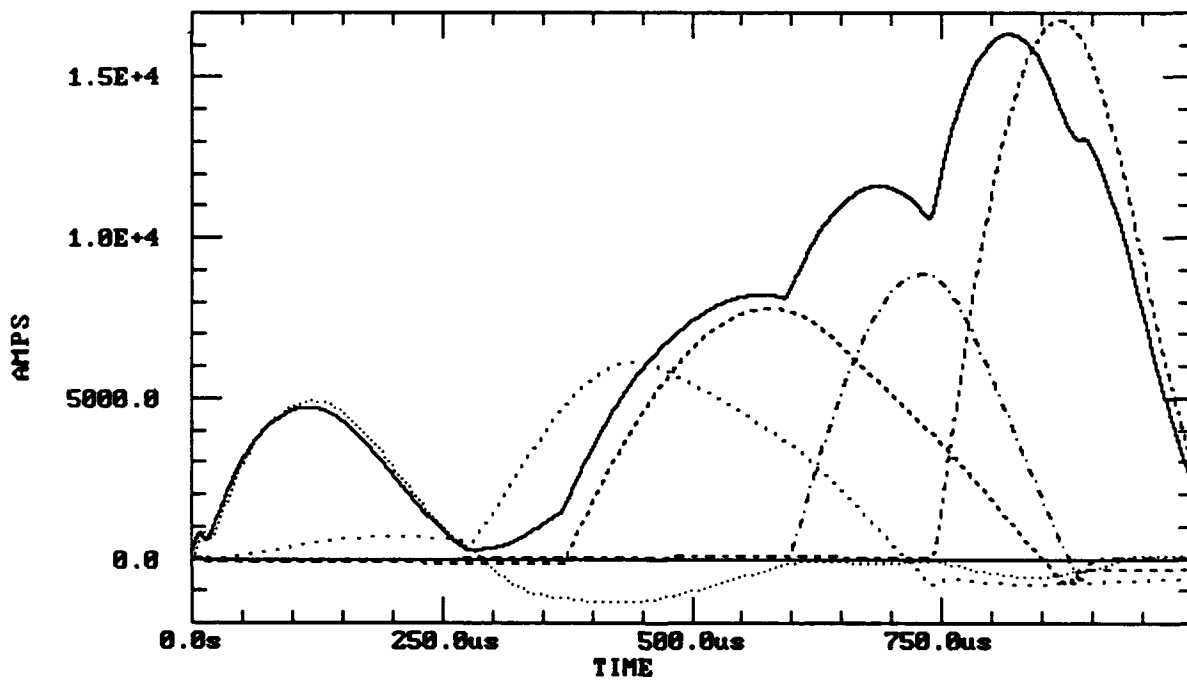


Figure 2. Current Profiles of Modules 1-5 With Switching at $t = 0, 280 \mu s, 370 \mu s, 597 \mu s,$ and $741 \mu s,$ Respectively. Solid Line Indicates Total Load Current.

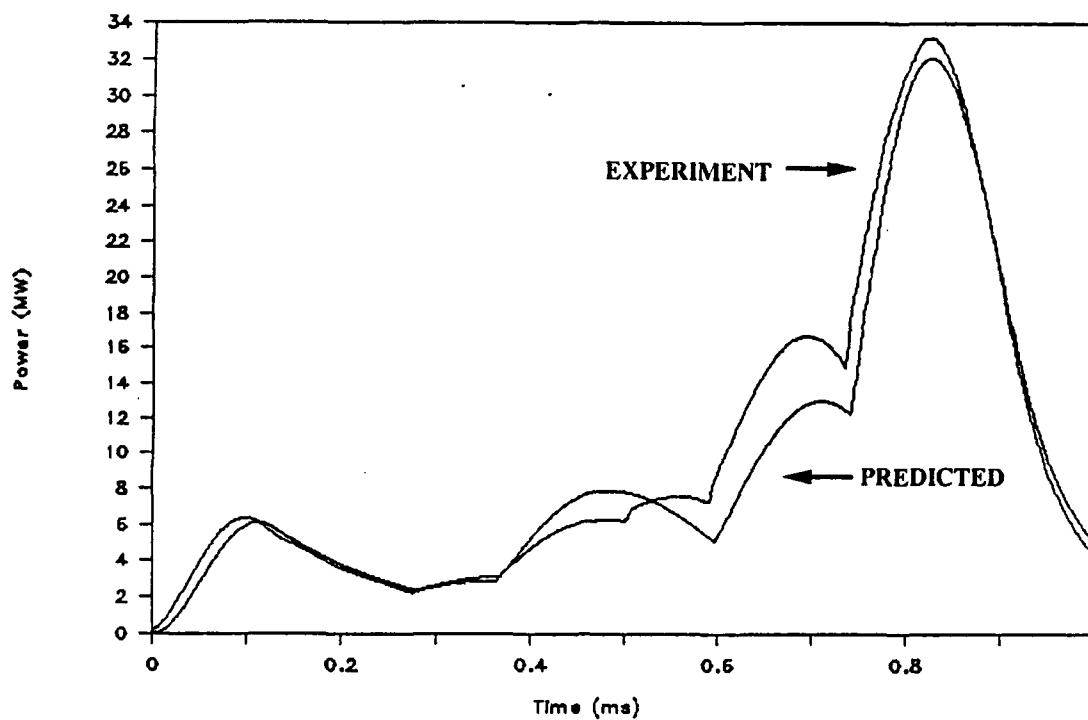


Figure 3. Power Profiles of 13-kJ Discharge to a 35-Milliohm Load.

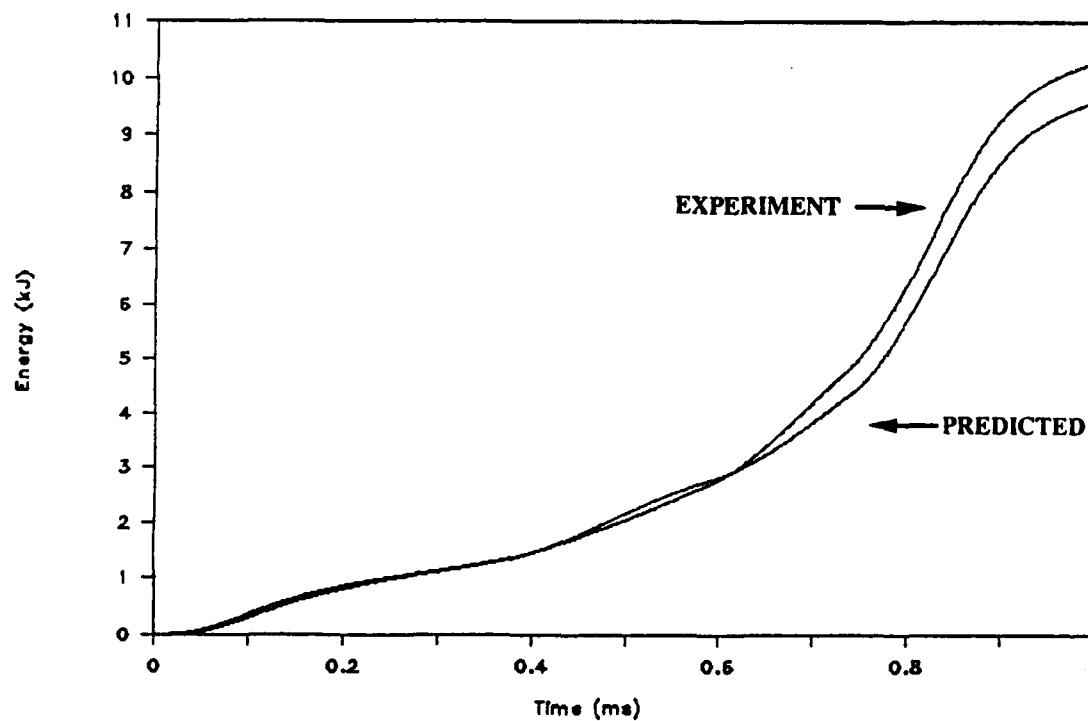


Figure 4. Energy Profiles of 13-kJ Discharge to a 35-Milliohm Load.

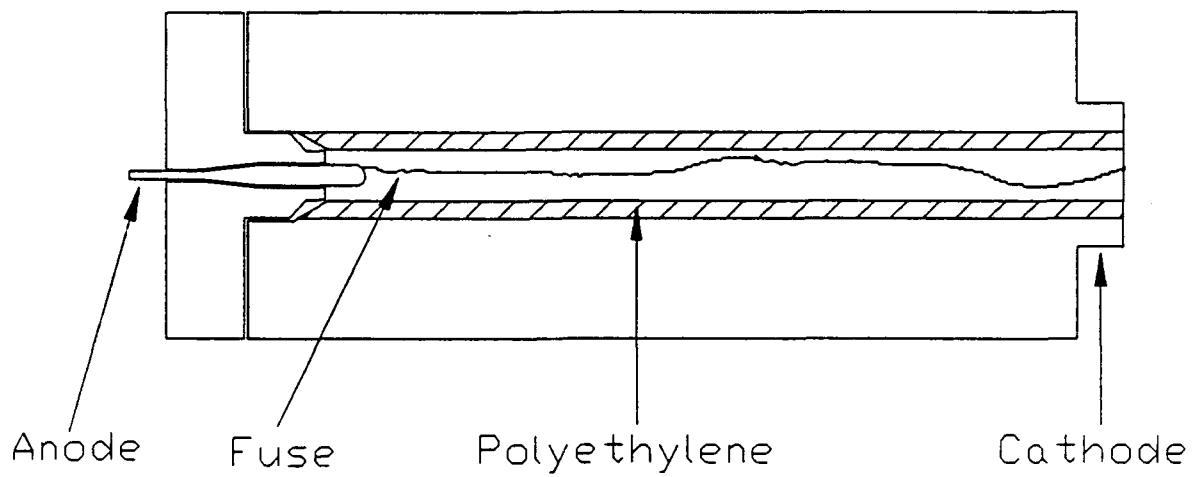


Figure 5. Diagram of Electrothermal-Gun Capillary Chamber.

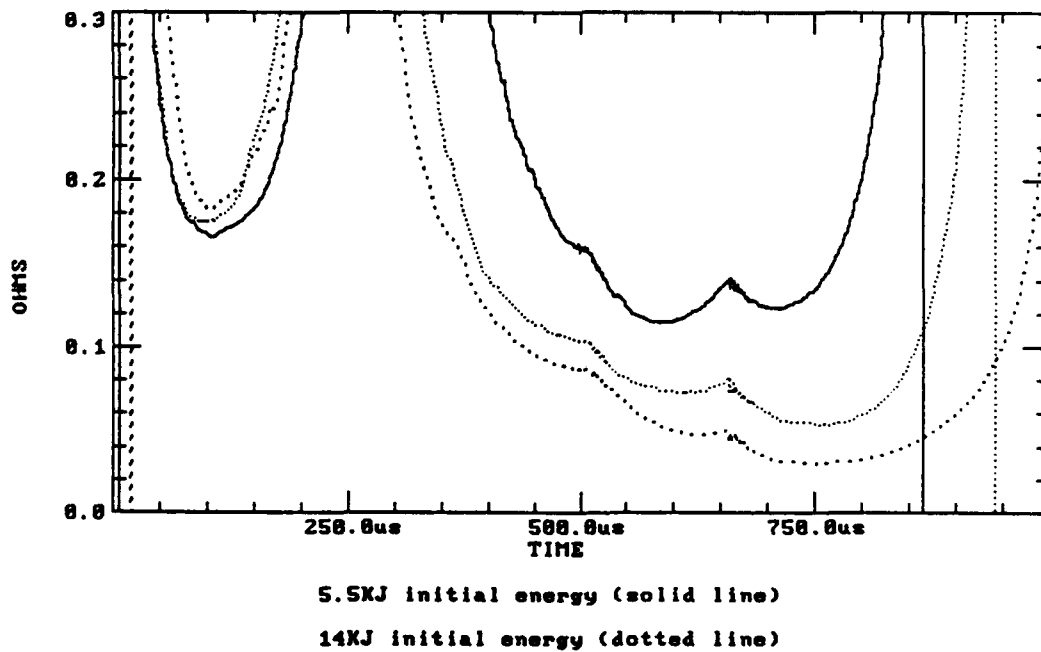


Figure 6. Resistance Curves of a Capillary With Length = 52.75 mm and Diameter = 9.45 mm.

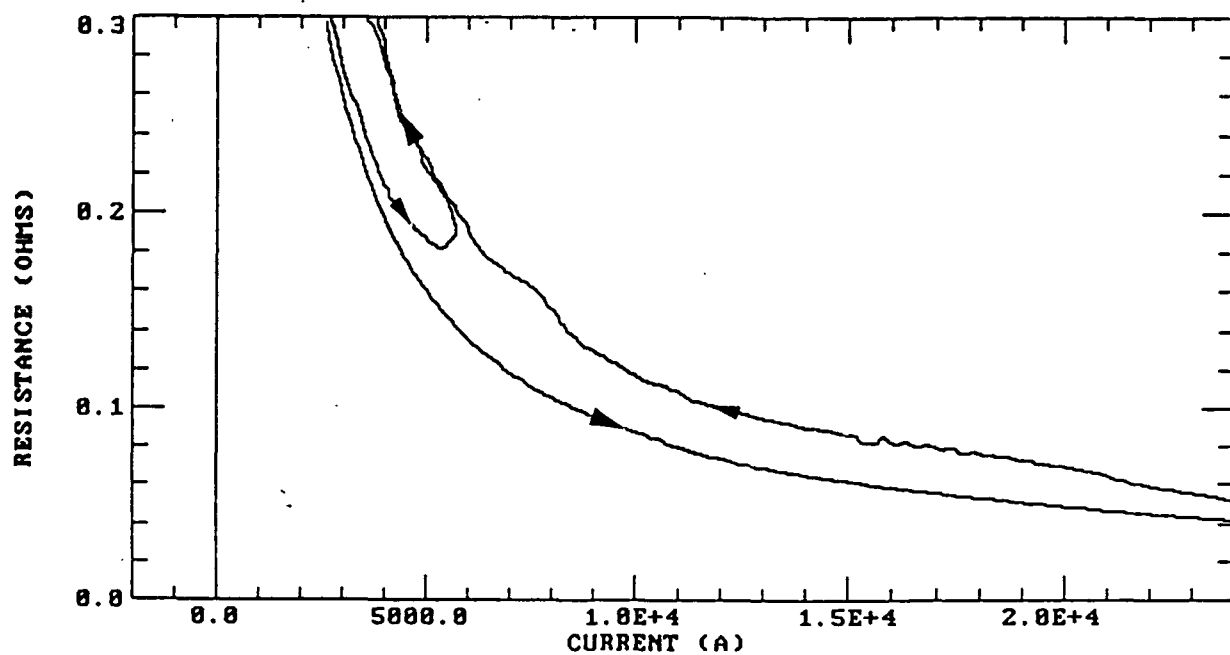


Figure 7. Resistance vs. Current of the 22-kJ Test in Figure 6.

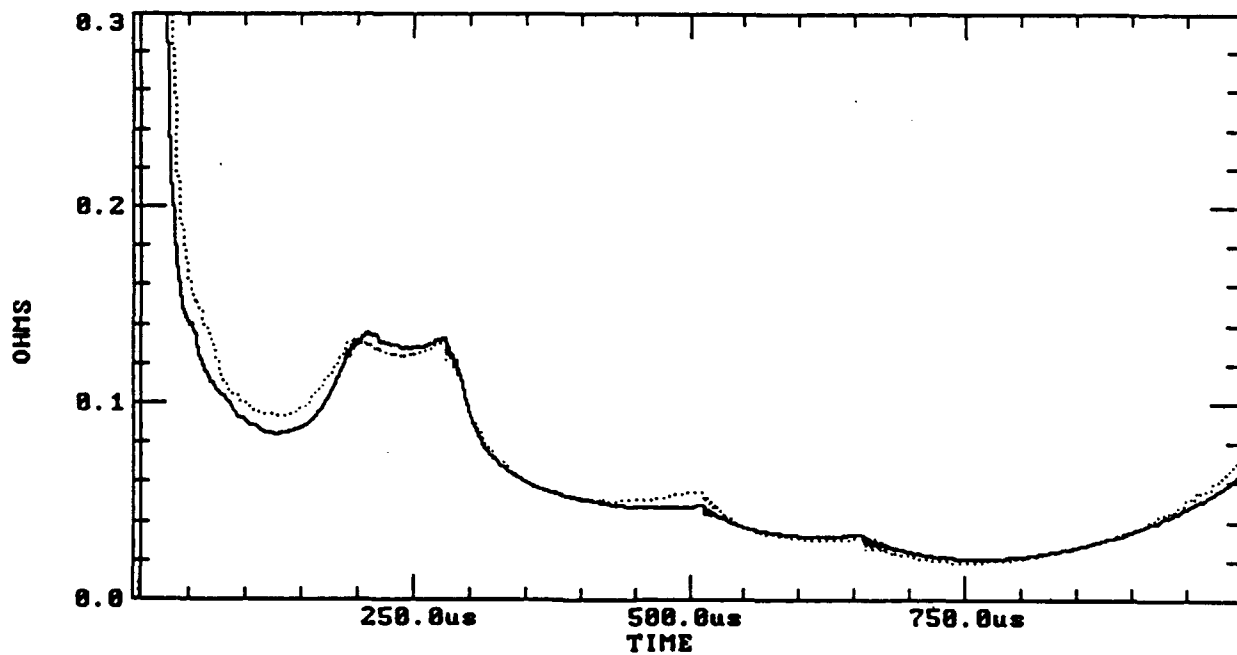


Figure 8. Resistance Curves of Capillary With Length = 52.75 mm and Diameter = 12.3 mm.

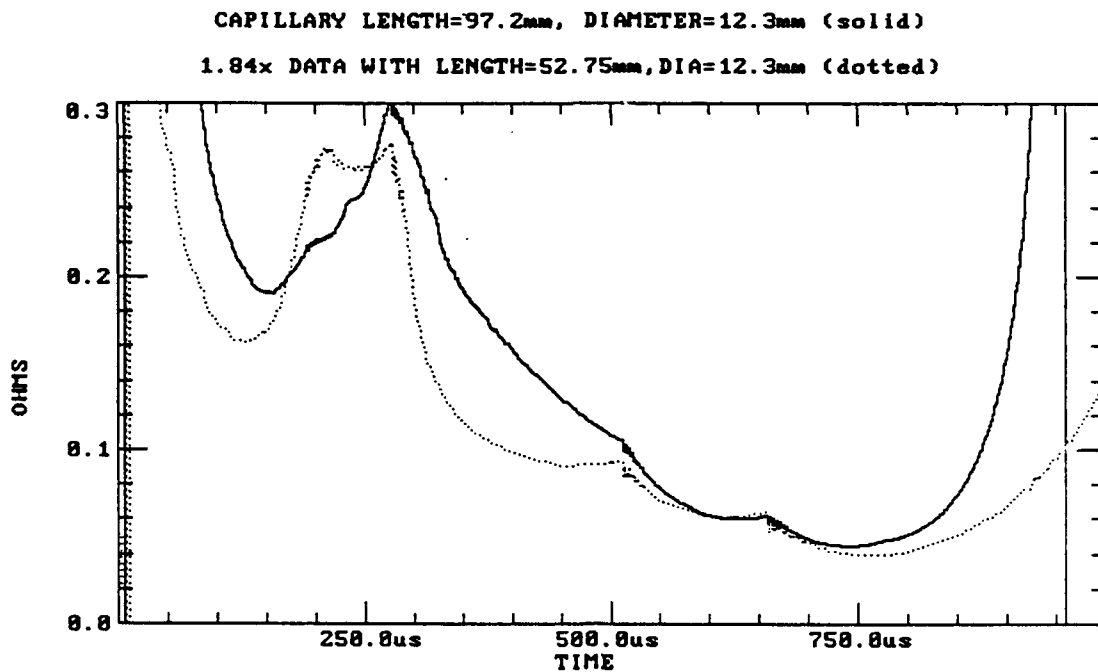


Figure 9. Resistance With Length = 97.2 mm and Diameter = 12.3 mm Compared to Scaled Figure 8.

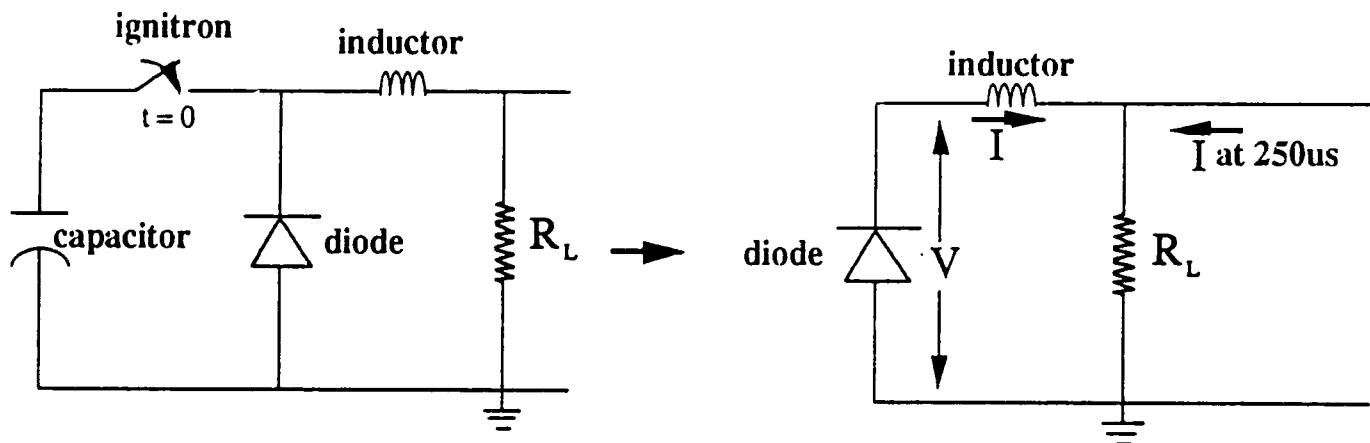


Figure 10. Two Module PFN With Second Module Triggered at 250 μ s. Circuit With a Diode Shunting Capacitor and Switch (a) and the Same Circuit With the Ignitron Extinguished (b).

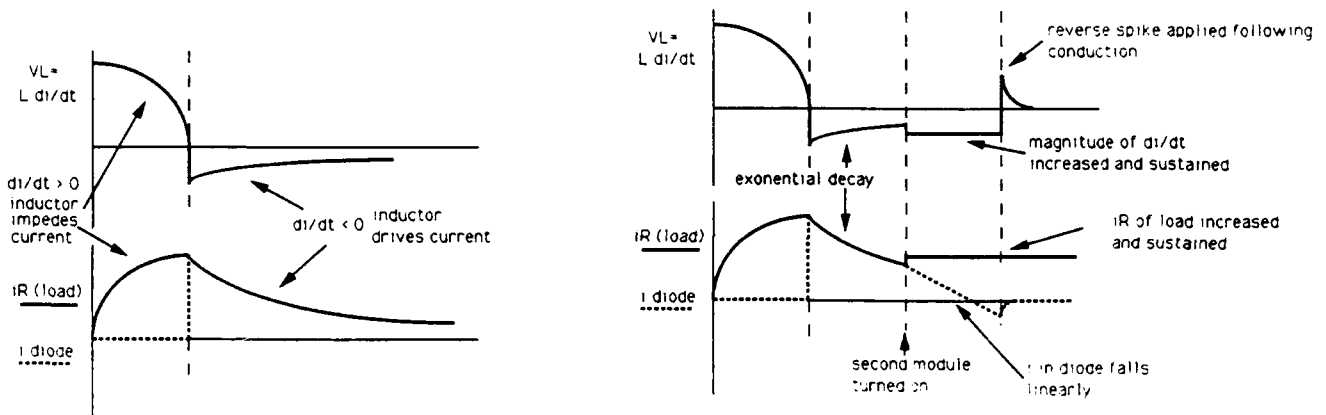


Figure 11. Theoretical Plots of Inductor Voltage (V_L), Load Voltage (iR), and Diode Current for the Circuit of Figure 10a Without a Second Module (a) and With a Second Module (b).

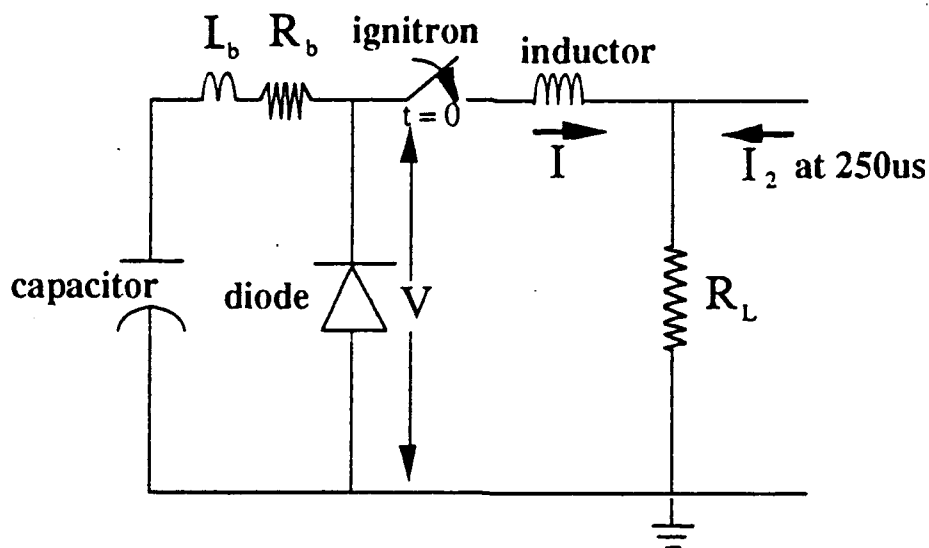


Figure 12. Diagram of Circuit With the Ignitron Switch Moved and the Diode Directly in Parallel With the Capacitor.

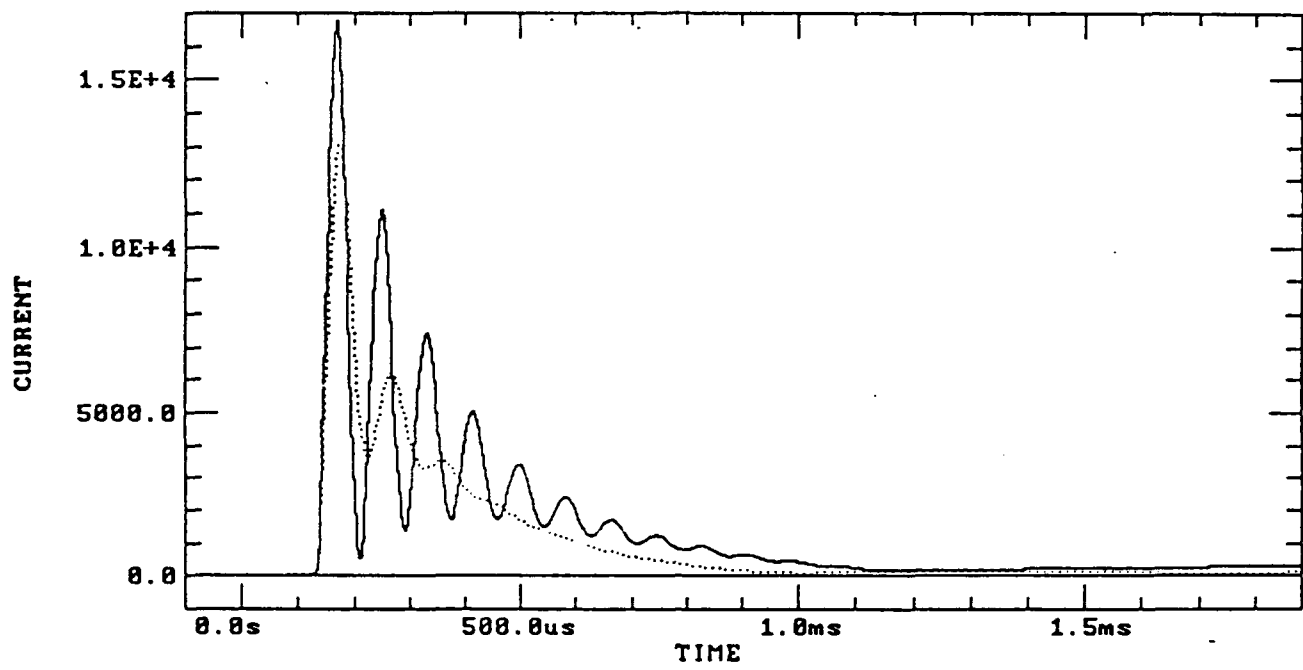


Figure 13. Measurement of Diode Current in Circuits With Two Degrees of Damping.

INTENTIONALLY LEFT BLANK.

4. REFERENCES

Glasoe, G. N., and J. V. Lebacqz. Pulse Generators. New York: McGraw-Hill, Inc., 1948.

Jamison, K. A., R. Stearns, and W. Fendley. "Damage Mechanisms of Crow-Bar Diodes in the 4.8 MJ Capacitor Bank." Technical Information Memorandum-1-326. SAIC, Shalimar, FL, January 31, 1990.

Powell, J. D., and A. E. Zielinski. "Analysis of the Plasma Discharge in an Electrothermal Gun." U.S. Army Ballistic Research Laboratory, Aberdeen Proving Ground, MD, unpublished.

INTENTIONALLY LEFT BLANK.

<u>No. of</u> <u>Copies</u>	<u>Organization</u>	<u>No. of</u> <u>Copies</u>	<u>Organization</u>
2	Administrator Defense Technical Info Center ATTN: DTIC-DDA Cameron Station Alexandria, VA 22304-6145	1	Commander U.S. Army Missile Command ATTN: AMSMI-RD-CS-R (DOC) Redstone Arsenal, AL 35898-5010
1	Commander U.S. Army Materiel Command ATTN: AMCAM 5001 Eisenhower Avenue Alexandria, VA 22333-0001	1	Commander U.S. Army Tank-Automotive Command ATTN: ASQNC-TAC-DIT (Technical Information Center) Warren, MI 48397-5000
1	Commander U.S. Army Laboratory Command ATTN: AMSLC-DL 2800 Powder Mill Road Adelphi, MD 20783-1145	1	Director U.S. Army TRADOC Analysis Command ATTN: ATRC-WSR White Sands Missile Range, NM 88002-5502
2	Commander U.S. Army Armament Research, Development, and Engineering Center ATTN: SMCAR-IMI-I Picatinny Arsenal, NJ 07806-5000	(Class. only) 1	Commandant U.S. Army Field Artillery School ATTN: ATSF-CSI Ft. Sill, OK 73503-5000
2	Commander U.S. Army Armament Research, Development, and Engineering Center ATTN: SMCAR-TDC Picatinny Arsenal, NJ 07806-5000	(Unclass. only) 1	Commandant U.S. Army Infantry School ATTN: ATSH-CD (Security Mgr.) Fort Benning, GA 31905-5660
1	Director Benet Weapons Laboratory U.S. Army Armament Research, Development, and Engineering Center ATTN: SMCAR-CCB-TL Watervliet, NY 12189-4050	1	Air Force Armament Laboratory ATTN: WL/MNOI Eglin AFB, FL 32542-5000
(Unclass. only) 1	Commander U.S. Army Armament, Munitions and Chemical Command ATTN: AMSMC-IMF-L Rock Island, IL 61299-5000	2	Dir, USAMSAA ATTN: AMXSY-D AMXSY-MP, H. Cohen
1	Director U.S. Army Aviation Research and Technology Activity ATTN: SAVRT-R (Library) M/S 219-3 Ames Research Center Moffett Field, CA 94035-1000	1	Cdr, USATECOM ATTN: AMSTE-TC
		3	Cdr, CRDEC, AMCCOM ATTN: SMCCR-RSP-A SMCCR-MU SMCCR-MSI
		1	Dir, VLAMO ATTN: AMSLC-VL-D
		10	Dir, BRL ATTN: SLCBR-DD-T

INTENTIONALLY LEFT BLANK.

USER EVALUATION SHEET/CHANGE OF ADDRESS

This laboratory undertakes a continuing effort to improve the quality of the reports it publishes. Your comments/answers below will aid us in our efforts.

1. Does this report satisfy a need? (Comment on purpose, related project, or other area of interest for which the report will be used.) _____

2. How, specifically, is the report being used? (Information source, design data, procedure, source of ideas, etc.) _____

3. Has the information in this report led to any quantitative savings as far as man-hours or dollars saved, operating costs avoided, or efficiencies achieved, etc? If so, please elaborate. _____

4. General Comments. What do you think should be changed to improve future reports? (Indicate changes to organization, technical content, format, etc.) _____

BRL Report Number BRL-TR-3304 Division Symbol _____

Check here if desire to be removed from distribution list. _____

Check here for address change. _____

Current address: Organization _____
 Address _____

DEPARTMENT OF THE ARMY

Director
U.S. Army Ballistic Research Laboratory
ATTN: SLCBR-DD-T
Aberdeen Proving Ground, MD 21005-5066

OFFICIAL BUSINESS

BUSINESS REPLY MAIL

FIRST CLASS PERMIT No 0001, APG, MD

Postage will be paid by addressee.

Director
U.S. Army Ballistic Research Laboratory
ATTN: SLCBR-DD-T
Aberdeen Proving Ground, MD 21005-5066



NO POSTAGE
NECESSARY
IF MAILED
IN THE
UNITED STATES

